Metagrating absorber: design and implementation

Fabrice Boust, Thomas Lepetit, Shah Nawaz Burokur

Metagrating absorber: Design and implementation

FABRICE BOUST,[1,*] THOMAS LEPETIT,[1] SHAH NAWAZ BUROKUR[2,*]

[1]*DEMR, ONERA, Université Paris-Saclay, F91123 Palaiseau, France*

[2]*LEME, UPL, Univ Paris Nanterre, F92410 Ville d'Avray, France*

**Corresponding author: fabrice.boust@onera.fr, sburokur@parisnanterre.fr*

The extent to which the introduction of subwavelength spatial modulation of electromagnetic properties improves absorption performances is studied. The proposed absorber represents an evolution from the Salisbury screen whereby the uniform resistive layer is replaced by a metagrating. A periodic supercell that supports only the specular reflection is first designed and load impedances are then engineered to suppress this diffraction mode. To experimentally demonstrate the concept, four prototypes are fabricated and tested in the microwave domain around 10 GHz. Furthermore, the performances assessed by a merit factor derived from Rozanov's bound show that the use of metagratings opens up good perspectives for improving the state of art. Our findings can pave the way towards the development of high performance absorbers for applications across a broad frequency spectrum.

Electromagnetic (EM) absorbers are of prime importance for applications related to radar cross section reduction, EM interference, EM compatibility, EM protection [1] as well as antennas for mutual coupling reduction [2]. Absorbers are traditionally designed by combining homogeneous layers. The intrinsic characteristics of these layers, such as thickness, electric permittivity or magnetic permeability, are selected to best suit the intended application. Conventional absorbers include Dällenbach structures [3], Salisbury screens [4] and Jaumann layers [5-6]. A homogeneous magnetodielectric layer placed over a ground plane is used to dissipate incident power in Dällenbach absorbers. The Salisbury screen, composed of a resistive sheet with tuned resistance placed at a distance of a quarter wavelength over a ground plane, is used to generate destructive interference in a narrow frequency band. To widen the absorption bandwidth, several Salisbury screens can be stacked over each other to form the Jaumann layer. A bound on the thickness to bandwidth ratio of absorbers was established in 2000 by K. Rozanov [7]. It is important to expess the bandwidth in terms of wavelength since the major difficulty is to achieve absorption at low frequencies with a minimum thickness.

Today, absorbing structure designs are mostly oriented toward the use of frequency selective surfaces (FSS).1 As such, high impedance surfaces (HIS) have been added to thin Salisbury screens to minimize reflectivity over a wide frequency band [8-9] Metasurfaces where the imaginary parts of the electromagnetic parameters are manipulated to enhance the tangent losses have also been employed to increase losses to create an efficient absorber [10-11]. In these approaches, structuring is carried out on a small scale with respect to wavelength and with a single type of pattern to consider the layers as homogeneous and assign them a uniform permittivity or effective impedance. Under these conditions, the performance of these absorbers is still subjected to Rozanov's bound. To enhance the performance of absorbers, the circuit analog (CA) absorber, further characterized by reactive components in addition to resistive sheets, provides an effective solution to overcome the problems of narrow bandwidth and high thickness [12-13]. As such, the CA absorber exploits the use of FSSs or metasurfaces loaded with lumped resistors.

The concept of metagratings has evolved from classical diffraction gratings and represents an interesting alternative to metasurfaces for wavefront manipulation [14]. However, there is only a limited number of meta-atoms in a metagrating supercell compared to the densely packed metasurface supercell incorporating numerous meta-atoms with subwavelength arrangement. Therefore, unlike metasurfaces, the sparse arrangement of the constituting scatterers does not make possible a description of metagratings in terms of surface impedances. A metagrating, an array of scatterers separated by a distance of the order of the operating wavelength, enables diffraction engineering by canceling a number of undesired propagating diffraction orders and keeping only desired ones for radiation. As such, perfect anomalous reflection and perfect beam splitting [14-20] mode conversion [21], orbital angular momentum beams [22] and near-field focusing [23-24] have been demonstrated with metagratings.

In this Letter, we propose to examine, to which extent, the modulation of electromagnetic properties at a scale smaller than the wavelength allows an increase in the absorption bandwidth.

Consequently, structures derived from the Salisbury screen by replacing the uniform resistive layer by a metagrating are studied here. The theoretical design is presented and validated by numerical simulations and experimental measurements for a 10 GHz operating frequency. The design of such metagrating absorber relies on the use of a periodic supercell that supports a single diffracted order, namely, the specular reflection and the aim is then to suppress this diffraction mode. The performances obtained from the proposed absorbing structure are further compared to a Salisbury screen of reference with the help of a merit factor derived from Rozanov's bound. A related study actually focuses on an analytical design methodology so as to show the influence of impedance density composition on the absorption bandwidth [25]. Such design concept is the key for future development of thin EM absorbers in various applications including, communication systems, stealth, camouflaging and noninvasive probing.

In a general manner, a metagrating is represented by a periodic array of supercells. Each supercell is itself composed of N thin wires. When the metagrating is illuminated by an incident plane wave, polarization line currents are excited in the wires, resulting in a scattered field represented by Floquet-Bloch modes defined by the period L of the supercell. As such, the diffraction angles of propagating orders θ_m can be found via the grating formula: $L(\sin\theta_m - \sin\theta) = m\lambda$, where m represents the number of an order and θ is the incidence angle of the illuminating plane wave. A line current is represented by the 2-D Dirac delta function $\delta(y,z)$ that allows analytically calculating the scattered field composed of both propagating and evanescent diffraction orders.

As presented in Fig. 1, we exploit a reflective metagrating where the load wires are on the top face of a grounded dielectric substrate. The wires are excited by a *TE*-polarized plane wave illumination, where $\exp(i\omega t)$ is assumed, and as detailed in Ref. [18], the complex amplitude A_m^{TE} of the electric field of the m^{th} diffracted plane wave is given by:

$$\boldsymbol{A_m^{TE}(k)} = -\frac{k\eta}{2L}\frac{(1+R_m^{TE})e^{i\beta_m h}}{\beta_m}\sum_{q=1}^{N} \boldsymbol{I_q} e^{i\xi_m(q-1)d} + \boldsymbol{\delta_{m0}} R_0^{TE} e^{2i\beta_0 h} \quad (1)$$

where k and η are, respectively, the wavenumber and the characteristic impedance in air. ξ_m and β_m are the tangential and normal components of the plane waves wavevector, respectively, and are calculated as $\xi_m = k\sin(\theta_i) + 2\pi m/L$ and $\beta_m = \sqrt{k^2 - \xi_m^2}$. R_m^{TE} is the corresponding Fresnel's reflection coefficient and is given by:

$$R_m^{TE} = \frac{i\gamma_m^{TE}\tan(\beta_m^s h) - 1}{i\gamma_m^{TE}\tan(\beta_m^s h) + 1} \quad (2)$$

with $\gamma_m^{TE} = \mu_s \frac{\beta_m}{\beta_m^s}$ and $\beta_m^s = \sqrt{\varepsilon_s \mu_s k^2 - \xi_m^2}$.

$N = M$ line currents I_q must be exploited in a supercell to control the complex amplitudes of the M propagating diffraction orders in a metagrating. However, active and/or lossy impedances are required for a perfect control [19]. As such, if there are enough wires per period and if the line currents I_q are engineered, it is possible to control the electric field reflected by the metagrating. I_q can be tailored by engineering the load-impedance density Z_q of each wire. These two quantities are related by Ohm's law, which is written as [26]:

$$\boldsymbol{Z_q I_q} = \boldsymbol{E_x^{exc}(y_q, -h)} - \boldsymbol{Z_{in} I_q} - \sum_{p=1}^{N} \boldsymbol{Z_{qp}^{(m)} I_p} \quad (3)$$

$E_x^{exc}(y_q, -h) = \left(e^{-i\beta_0 z} + R_0^{TE} e^{i\beta_0(z+2h)}\right) e^{-ik\sin(\vartheta) y_q}$ is the external electric field created by the incident wave and reflected from the grounded substrate and $Z_{in} = k\eta H_0^{(2)}[kr_0]/4$ is the input-impedance density of the wire. $Z_{qp}^{(m)}$ are the mutual-impedance densities corresponding to the interaction with the other wires and depend only on the geometry of the wires.

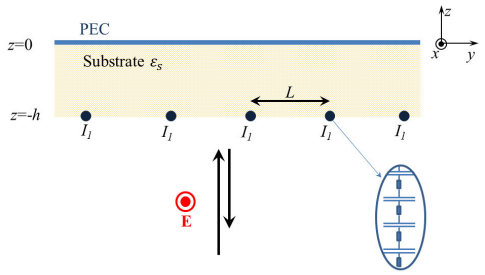

Fig. 1. Schematic principle of the metagrating absorber implemented by a single load wire per period ($N = 1$).

The load-impedance density Z_q can be calculated using the electromagnetic simulation-based local periodic approximation (LPA) approach proposed in Ref. [27]. Full-wave simulations are first performed on an elementary cell placed in an infinite array by applying periodic boundary conditions and illuminated by an incident plane wave to calculate the reflection coefficient. In such configuration, the cell size being of subwavelength scale limits reflection to the specular term. Assuming small diameter wires, the reflection coefficient obtained from simulations is then used to analytically calculate Z_q, by subtracting the mutual impedance density due to effects of the interactions between wires and geometrical parameters such as substrate's thickness. It is thus possible to associate a three-dimensional design of an elementary cell and a load impedance, to be used in any metagrating.

In this study, we consider a Salisbury-like screen composed of a 3 mm thick grounded dielectric substrate of relative permittivity $\varepsilon_s = 2.2$ and a metagrating layer with 1 line current per supercell in a first step, required to cancel the specular reflection at a single frequency. For the sake of simplicity, we consider normal incidence illumination. The length L of the supercell is chosen to be $L < \lambda$ such that only the 0^{th} diffracted order, which is the specular reflection, is present. Equation (1) can then be written as:

$$\boldsymbol{A_0^{TE}(k)} = -\frac{\eta}{2L}(\mathbf{1} + \boldsymbol{R_0^{TE}})e^{ikh}\sum_{q=1}^{N}\boldsymbol{I_q} + \boldsymbol{R_0^{TE}} e^{2ikh} \quad (4)$$

with $k = \frac{2\pi f}{c}$.

Solving analytically (3) allows expressing the current I_q as a function of Z_q. The currents I_q is then injected into (4), which expresses the amplitude of the specular reflection in terms of the impedance densities Z_q. Besides, our main goal is to further expand the absorption frequency bandwidth. Hence, several frequency points are targeted and a supplemental wire is engineered for each additional frequency by considering the limited number N of wires that can be placed in the same supercell of length L. Since (4) must be written for several frequencies, it is necessary to have an impedance model with frequency-independent parameters. Here,

Table I. Parameters and performances of metagrating structures with different number of wires.

N	r_q (Ω/m)	c_q (fF.m)	Cell design (capacitances and resistances)	δ (mm)	A (mm)	r (Ω)	L_r (nH)	C_r (fF)	BFM (Analytical) -10 dB	BFM (Analytical) -15 dB	BFM (Experimental) -10 dB	BFM (Experimental) -15 dB
1	8530	0.26	2 C + 1 R	10	2.2	50	0.9	100	0.03	0.024	0.052	0.027
2	11190	0.20	2 C + 1 R	8	2.4	50	0.9	100	0.13	0.15	0.15	0.15
	8790	0.29	2 C + 1 R	8	3.5	50	0.9	100				
3	3860	0.17	2 C + 1 R	8	1.8	18	0.4	60	0.15	0.18	0.21	0.26
	10420	0.32	2 C + 1 R	8	3.85	50	0.9	100				
	12210	0.22	2 C + 1 R	8	2.6	50	0.9	100				
4	10885	0.33	2 C + 1 R	8	4.0	50	0.9	100	0.25	0.33	0.12	0
	5340	0.14	2 C + 1 R	8	1.5	25	0.45	70				
	23380	0.21	2 C + 1 R	8	2.7	100	0.9	100				
	120	0.14	1 C	8	4.2	-	-	-				
Salisbury									0.20	0.16		

we consider a load impedance composed of a resistance and a capacitance:

$$\boldsymbol{Z_q = r_q - \frac{i}{c_q 10^{-15} \omega}} \quad (5)$$

where r_q and c_q are expressed in Ω/m and fF.m, respectively. For N = 1, r_1 et c_1 can be found algebraically. For N = 2, 3 and 4, Eq. (4) is written for a set of frequencies $\{f_i\}$ chosen to maximize the bandwidth around 10 GHz with a magnitude of -15 dB. r_q and c_q are determined to reach a minimum for the quantity $\sum_{\{f_i\}} |A_0^{TE}(f_i)|$. Table I shows the values of r_q and c_q calculated for four structures, where each structure only differs by the number of wires N. The size L of the supercell is calculated to be 20 mm and the distance between two wires is L/N.

To engineer the calculated impedances, the elementary cell composed of two microstrip capacitances in series with a lumped resistance is selected, as illustrated in the photograph of the N = 1 fabricated metagrating sample in Fig. 2. The impedance densities are calculated for a set of values of resistance r between 10 and 100 Ω and width A between 1 mm and 5 mm for two values of δ(8 mm and 10 mm). The gap in the microstrip capacitances is fixed to 0.25 mm. By interpolation, the different widths and resistance values leading to the required impedances are determined. For the resistances, commercially available components are used. In the analytical calculations, the resistors are assumed to be perfect and the metal pads to be infinitely conductive, while in full-wave numerical simulations, a *RLC* model is used. A simple model composed of an inductance in series with the resistance and a capacitance in parallel is considered [28]. Table I summarizes the different values of δ and A as well as the different components values r, L_r and C_r in the resistances. The period δ along the x-direction is chosen so that the commercially available resistance values are not too far from the calculated ones, with a difference of less than 15%.

To verify the performances of the designed metagrating absorbers, full-wave simulations based on the finite-element method (FEM) technique using COMSOL Multiphysics are conducted. For experimental tests, reflection measurements are performed on samples having dimensions 140 mm × 140 mm in a microwave anechoic chamber dedicated to radar-cross-section bistatic measurements, where transmitting and receiving horn antennas are mounted on a circular track of 5 m radius. The transmitter is fixed at -2° and the receiver is fixed at +2°, as schematically illustrated in the inset of Fig. 2. The different reflection coefficients are shown in Fig. 3. To evaluate the obtained performances, we use a factor of merit derived from Rozanov's bound for non-magnetic materials. In Ref. [7], K Rozanov establishes that the thickness of a non-magnetic broadband absorbing screen with a reflection coefficient less than Γ_{dB} on a continuous wavelength $\Delta\lambda$, is necessarily greater than:

$$\boldsymbol{d_{Rozanov} = \frac{\ln(10)}{40\pi^2} \Delta\lambda \, |\Gamma_{dB}|} \quad (6)$$

Consequently, the performance of the designed absorbing screens is evaluated by a factor of merit defined as the ratio of the Rozanov's thickness to the effective thickness of the screen:

$$\boldsymbol{BFM(\Gamma_{dB}) = \frac{d_{Rozanov}}{d} = \frac{\ln(10)}{40\pi^2} \frac{|\Gamma_{dB}| \, \Delta\lambda}{d}} \quad (7)$$

Such factor of merit, necessarily lower than unity for non-magnetic structures, makes possible a comparison of the performances of absorbing screens that operate at different frequency bands and for different levels of absorption, as shown in Table I.

As illustrated in Table I, the BFM is extracted for two different levels of absorption. The best performance is obtained for the experimental 3-wires metagrating absorber with a factor of merit of 0.26 compared to 0.16 for the analytically calculated Salisbury screen of similar thickness. A qualitative agreement is obtained between simulations and experiments provided that the resistance parasitic terms are taken into account in simulations. The slight residual frequency shift between 3D numerical simulations with parasitic terms and experiments is due to the model used for the resistors that does not take into account the welding of the pads and also to the dispersion of the components. In addition, the LPA

method used to calculate impedance densities takes into account the interactions between wires assuming that they are equivalent to infinitely thin wires. This approximation is less and less valid as the number of wires in a supercell increases. This is one of the hypotheses with the dispersion of resistance characteristics that could explain the poor performance of the 4-wires absorber.

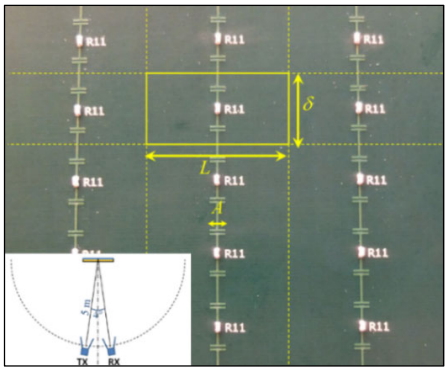

Fig. 2. Photograph of a fabricated sample composed of one wire per supercell (N = 1). The geometrical dimensions are: L = 20 mm, δ = 10 mm and A = 2.2 mm. The gap in the microstrip capacitances is 0.25 mm. The resistance value is 50 Ω.

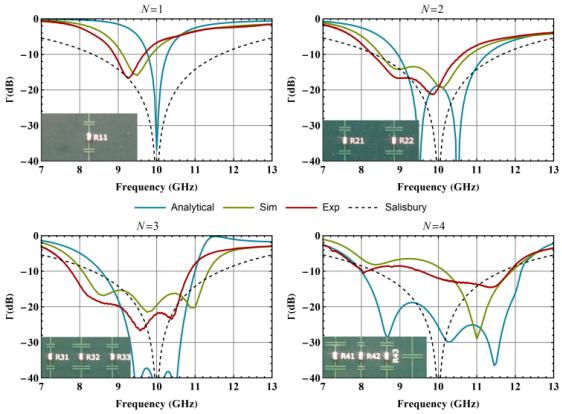

Fig. 3. Performances in terms of reflection coefficients for different metagrating structures composed of N = 1, 2, 3 and 4 load wires. Theoretical calculations, numerical simulations and experimental measurements are shown and compared to the performance of a Salisbury screen of similar thickness.

In conclusion, the impedance modulation induced by the designed metagrating structures achieves a better performance than the Salisbury screen, particularly when high level of absorption is desired. For a relevant comparison with widely developed metasurface-based absorbers, improvements on the proposed metagrating are necessary, such as by stacking several layers and by considering an elaborated load impedance model. In this work, the proposed metagrating abosrber concept is validated for a single polarization, but can be further extended to two simultaneous polarizations by combining two perpendicular wire arrays. Finally, the approach can be extended to metagratings with several diffracted orders and also to multilayer systems, in analogy to a Salisbury screen with a front-facing impedance matching layer, which would possibly lead to wider absorption bandwidth. It would be then necessary to replace the lumped resistors by resistive layers to facilitate their integration.

Disclosures. The authors declare no conflicts of interest.

Data availability. Data underlying the results presented in this paper are not publicly available at this time but may be obtained from the authors upon reasonable request.

References

1. B. Munk, Frequency Selective Surfaces: Theory and Design (Wiley, 2005).
2. F. Yang and Y. Rahmat-Samii, IEEE Trans Antennas Propag. 51, 2936 (2003).
3. W. Dällenbach and W. Kleinsteuber, Hochfreq. u Elektroak 51, 152 (1938)
4. W. Salisbury, U.S. patent 2599944A (1952).
5. B. Chambers and A. Tennant, Electron. Lett. 30, 1530 (1994).
6. E. Knott and C. Lunden, IEEE Trans. Antennas Propag. 43, 1339 (1995).
7. K. N. Rozanov, IEEE Trans. Antennas Propag. 48, 1230 (2000).
8. O. Luukkonen, F. Costa, A. Monorchio, and S. A. Tretyakov, IEEE Trans. Antennas Propag. 57, 3119 (2009).
9. F. Costa, A. Monorchio, and G. Manara, IEEE Trans. Antennas Propag. 58, 1551 (2010).
10. N. I. Landy, S. Sajuyigbe, J. J. Mock, D. R. Smith, and W. J. Padilla, Phys. Rev. Lett. 100, 207402 (2008).
11. Y. Ra'di, C. R. Simovski, and S. A. Tretyakov, Phys. Rev. Appl. 3, 037001 (2015).
12. B. Munk, P. Munk, and J. Pryor, IEEE Trans. Antennas Propag. 55, 186 (2007).
13. L. Sun, H. Cheng, Y. Zhou, and J. Wang, Opt. Express 20, 4675 (2012).
14. Y. Ra'di, D. L. Sounas, and A. Alù, Phys. Rev. Lett. 119, 067404 (2017)
15. A. Epstein and O. Rabinovich, Phys. Rev. Appl. 8, 054037 (2017).
16. O. Rabinovich and A. Epstein, IEEE Trans. Antennas Propag. 66, 4086 (2018).
17. O. Rabinovich, I. Kaplon, J. Reis, and A. Epstein, Phys. Rev. B 99, 125101 (2019)
18. V. Popov, F. Boust, and S. N. Burokur, Phys. Rev. Appl. 10, 011002 (2018).
19. V. Popov, F. Boust, and S. N. Burokur, Phys. Rev. Appl. 11, 024074 (2019).
20. V. Popov, F. Boust, and S. N. Burokur, IEEE Trans. Antennas Propag. 68, 1533 (2020).
21. V. K. Killamsetty and A. Epstein, Phys. Rev. Appl. 16, 014038 (2021).
22. K. Zhang, Y. Wang, S. N. Burokur, and Q. Wu, IEEE Trans. Microwave Theory Tech. 70, 200 (2022).
23. V. Popov, B. Ratni, S. N. Burokur, and F. Boust, Adv. Opt. Mater. 9, 2001316 (2021).
24. O. Rabinovich and A. Epstein, Appl. Phys. Lett. 118, 131105 (2021).
25. Z. Tan, J. Yi, Q. Cheng, S. N. Burokur, IEEE Trans. Antennas Propag., under review.
26. S. Tretyakov, Analytical modeling in applied electromagnetics. Artech House, 2003.
27. V. Popov, M. Yakovleva, F. Boust, J.-L. Pelouard, F. Pardo, and S. N. Burokur, Phys. Rev. Appl. 11, 044054 (2019).
28. For more details on the CH0402 resistances. https://www.vishay.com/doc?53014.

References

1. B. Munk, Frequency Selective Surfaces: Theory and Design (Wiley, 2005).
2. F. Yang and Y. Rahmat-Samii, "Microstrip antennas integrated with electromagnetic band-gap (EBG) structures: a low mutual coupling design for array applications," IEEE Trans. Antennas Propag. 51, 2936 (2003).
3. W. Dällenbach, W. Kleinsteuber, "Reflection and absorption of decimeter-waves by plane dielectric layers," Hochfreq. u Elektroak 51, 152-156 (1938)
4. W. Salisbury, "Absorbent body of electromagnetic waves," U.S. patent 2599944A (10 June 1952).
5. B. Chambers, A. Tennant, "Design of wideband Jaumann radar absorbers with optimum oblique incidence performance," Electron. Lett. 30(18), 1530–1532 (1994).
6. E. Knott and C. Lunden, "The two-sheet capacitive Jaumann absorber," IEEE Trans. Antennas Propag. 43(11), 1339–1343 (1995).
7. K. N. Rozanov, "Ultimate thickness to bandwidth ratio of radar absorbers," IEEE Trans. Antennas Propag. 48, pp. 1230-1234 (2000).
8. O. Luukkonen, F. Costa, A. Monorchio, S.A. Tretyakov, "A thin electromagnetic absorber for wide incidence angles and both polarizations," IEEE Trans. Antennas Propag. 57, 3119-3125 (2009).
9. F. Costa, A. Monorchio, G. Manara, "Analysis and Design of Ultra Thin Electromagnetic Absorbers Comprising Resistively Loaded High Impedance Surfaces," IEEE Trans. Antennas Propag. 58, 1551-1558 (2010).
10. N.I. Landy, S. Sajuyigbe, J.J. Mock, D.R. Smith, W.J. Padilla, "Perfect Metamaterial Absorber," Phys. Rev. Lett. 100, 207402 (2008).
11. Y. Ra'di, C. R. Simovski, and S. A. Tretyakov, "Thin Perfect Absorbers for Electromagnetic Waves: Theory, Design, and Realizations," Phys. Rev. Appl. 3, 037001 (2015).
12. B. Munk, P. Munk, J. Pryor, "On designing Jaumann and circuit analog absorbers (CA absorbers) for oblique angle of incidence," IEEE Trans. Antennas Propag. 55(1), 186–193 (2007).
13. L. Sun, H. Cheng, Y. Zhou, J. Wang, "Broadband metamaterial absorber based on coupling resistive frequency selective surface," Opt. Express 20(4), 4675–4680 (2012).
14. Y. Ra'di, D. L. Sounas, A. Alù, "Metagratings: Beyond the limits of graded metasurfaces for wave front control," Phys. Rev. Lett. 119, 067404 (2017).
15. A. Epstein and O. Rabinovich, "Unveiling the properties of metagratings via a detailed analytical model for synthesis and analysis," Phys. Rev. Appl. 8, 054037 (2017).
16. O. Rabinovich, A. Epstein, "Analytical design of printed circuit board (PCB) metagratings for perfect anomalous reflection," IEEE Trans. Antennas Propag. 66, no. 8, pp. 4086–4095 (2018).
17. O. Rabinovich, I. Kaplon, J. Reis, A. Epstein, "Experimental demonstration and in-depth investigation of analytically designed anomalous reflection metagratings," Phys. Rev. B 99, 125101 (2019).
18. V. Popov, F. Boust, S. N. Burokur, "Controlling diffraction patterns with metagratings," Phys. Rev. Appl. 10, 011002 (2018)
19. V. Popov, F. Boust, S. N. Burokur, "Constructing the near field and far field with reactive metagratings: Study on the degrees of freedom," Phys. Rev. Appl., vol. 11, 024074 (2019).
20. V. Popov, F. Boust, S. N. Burokur, "Beamforming with metagratings at microwave frequencies: design procedure and experimental demonstration," IEEE Trans. Antennas Propag. 68, no. 3, pp. 1533-1541 (2020).
21. V. K. Killamsetty, A. Epstein, "Metagratings for Perfect Mode Conversion in Rectangular Waveguides: Theory and Experiment," Phys. Rev. Appl. 16, 014038 (2021).
22. K. Zhang, Y. Wang, S. N. Burokur, Q. Wu, "Generating dual-polarized vortex beam by detour phase: from phase gradient metasurfaces to metagratings," IEEE Trans. Microwave Theory Tech. 70(1), 200-209 (2022).
23. V. Popov, B. Ratni, S. N. Burokur, F. Boust, "Non-local reconfigurable sparse metasurface: Efficient near-field and far-field wavefront manipulations," Adv. Opt. Mater. 9, 2001316 (2021).
24. O. Rabinovich, Ariel Epstein, "Nonradiative subdiffraction near-field patterns using metagratings," Appl. Phys. Lett. 118, 131105 (2021).
25. Z. Tan, J. Yi, Q. Cheng, S. N. Burokur, "Design of perfect absorber based on metagrating: theory and experiment," IEEE Trans. Antennas Propag., under review.
26. S. Tretyakov, Analytical modeling in applied electromagnetics. Artech House, 2003.
27. V. Popov, M. Yakovleva, F. Boust, J.-L. Pelouard, F. Pardo, S. N. Burokur, "Designing metagratings via local periodic approximation: From microwaves to infrared," Phys. Rev. Appl. 11, 044054 (2019).
28. For more details on the CH0402 resistances. https://www.vishay.com/doc?53014.